

Influence of precursor thiourea contents on the properties of spray deposited Cu₂FeSnS₄ thin films

Santosh G. Nilange, Nandkishor M. Patil, Abhijit A. Yadav*

Thin Film Physics Laboratory, Department of Physics, Electronics and Photonics, Rajarshi Shahu Mahavidyalaya, Latur (Autonomous), 413512, Maharashtra, India



ARTICLE INFO

Keywords:
Spray pyrolysis
X-ray diffraction
Semiconducting materials
Optical properties
Electrical properties

ABSTRACT

Semiconducting Cu₂FeSnS₄ (CFTS) thin films were spray-deposited with different thiourea contents in the precursor solution. The influence of thiourea contents (10–14 ml) in the precursor solution on the crystallographic, morphological, compositional, optical, electrical and thermoelectrical properties of CFTS films was studied. X-ray diffraction analysis confirmed stannite phase having tetragonal crystal structure. The surface of CFTS thin films had hexagonal crystals. Nearly stoichiometric deposition has been witnessed through energy dispersive X-ray spectroscopy. Optical bandgap was found to be in the range 1.54–1.76 eV based on the different thiourea contents in the precursor solution. The considerable reduction in electrical resistivity has been observed for TH13 sample. The CFTS thin films are p-type as confirmed from thermoelectrical analysis.

1. Introduction

The increasing energy demand for the sustainable development and limited access to the energy sources, has forced us to look for the renewable energy sources [1]. Solar is the most economical, effective and inexhaustible source amongst the available energy resources [2]. One of the most auspicious alternatives to the world's energy crisis is to convert sun radiation into electrical energy [3,4]. A best and standard approach of conversion is the direct production of electric current from captured sunlight using solar photovoltaic cells [5,6].

There is a growing curiosity in transition metal chalcogenide thin films for solar cell applications because of their unique physical and chemical properties [7]. Copper indium gallium selenide (CIGS) and cadmium telluride (CdTe) thin films are favourable as absorber layers [8,9]. The CIGS based solar cell had shown an efficiency of 22.6%, however toxic selenium and expensive indium and gallium limits the development of solar cells [10,11]. However due to non-toxic constituents and earth abundance stannite Cu₂FeSnS₄ (CFTS) is promising photovoltaic material. CFTS have proper optical bandgap (1.20–1.54 eV) and high (10^4 cm^{-1}) absorption coefficient [12–16].

Zhang et al. [12] have synthesized CFTS nanocrystals with tunable bandgap of 1.46–1.54 eV. Yan and colleagues [13] have prepared tetragonal CFTS nanocrystals by a simple hot-injection method. Using the solvothermal method, Jiang and co-workers [14] have synthesized CFTS particles as absorber layer. Boutebakh et al. [17] have studied the effect of Zn molarity on the properties of p-type Cu₂ZnSnS₄ films. Agasti

and colleagues [18] have discussed the understanding Cu–Zn–Sn through electrodeposition.

In recent times, numerous physical and chemical techniques are employed for preparing CFTS including sputtering [19], solution growth [12], hot injection [13], solvothermal [14,20], spin coating [21], microwave [22], solid state reactions [23] and spray pyrolysis [24,25]. However most of the techniques used for preparing CFTS are time consuming and complex. The selection of the particular technique depends on different factors including precursors to be used, the type of the substrate, area of the films, application and structure of the film [25]. Amongst these, spray pyrolysis is most popular, eco-friendly, less expensive, non-vacuum with easy control over deposition rate, operates at moderate temperatures, and can be engaged for large area deposition [24,25].

Even though literature emphasise on growth and characterization of CFTS thin films using spray pyrolysis, the effects of thiourea contents in the precursor solution on the properties of spray deposited CFTS thin films have not been reported yet. Previously, CFTS thin films have been spray deposited at different deposition temperatures (175°C–325 °C). It is observed the CFTS film have a band gap of 1.54 eV. The room temperature resistivity is found to be $0.646 \times 10^5 \Omega\text{cm}$ [26]. By considering our goal to use these films for solar cell applications, we have decided to vary the thiourea contents in the precursor solution to enhance the CFTS film properties.

* Corresponding author.

E-mail address: aay_physics@yahoo.co.in (A.A. Yadav).

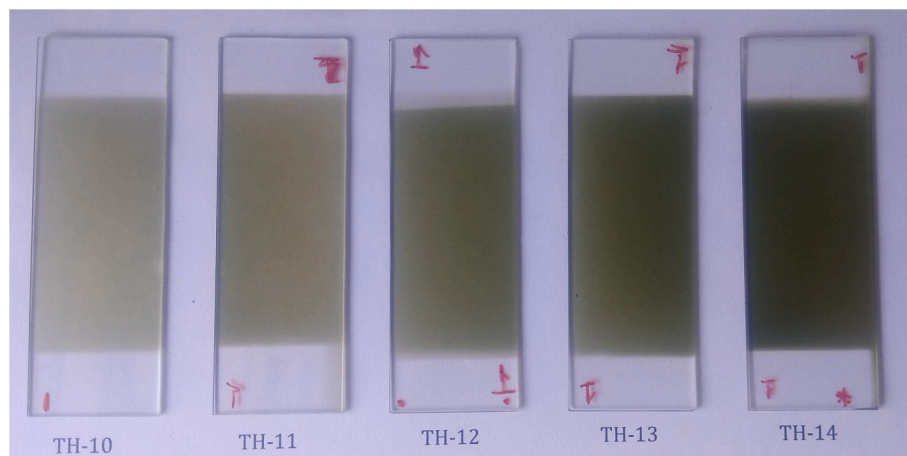


Fig. 1. Photograph of CFTS thin films spray deposited on glass with various thiourea contents in the precursor solution.

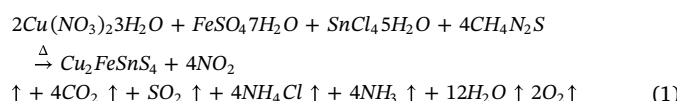
2. Experimental

The precursor solution was obtained by mixing copper nitrate (0.025 M), ferrous sulphate (0.025 M), stannic chloride (0.025 M) and thiourea (0.025 M) solutions. For first set of experiment, the final spraying solution was obtained by mixing 10 ml of Cu, Fe and Sn with 10 ml of S to obtain the Cu:Fe:Sn:S ratio as 2:1:1:4. For second set of experiment (TH11 sample), the final spraying solution was obtained by mixing 10 ml of Cu, Fe and Sn with 11 ml of S. Similarly for third set of experiment (TH12 sample), the final spraying solution was obtained by mixing 10 ml of Cu, Fe and Sn with 12 ml of S. In this fashion the CFTS films were deposited by varying the thiourea contents in the precursor solution at the interval of 1 ml from 10 ml to 14 ml to produce TH10, TH11, TH12, TH13 and TH14 samples of CFTS thin films, respectively. The films are deposited at optimized temperature of 250 °C. Spray rate was 3 ml min⁻¹. The nozzle to substrate distance was 30 cm. Air was used as carrier gas at pressure of 1.8 kg cm⁻².

The film thicknesses of CFTS were determined through gravimetric weight difference method. The crystallographic parameters were obtained via X-ray diffraction (XRD) pattern recorded using Philips PW-3710 X-ray diffractometer with Cu-k_α radiation ($\lambda = 1.54056 \text{ \AA}$). Surface morphological and compositional investigation was performed with JEOL-JSM-6360A analytical scanning electron microscope (SEM). The optical absorption spectra of CFTS thin films were obtained in the 450–1050 nm wavelength range using UV-Vis spectrophotometer (SHIMADZU UV-1700), and further used to determine the bandgap energy and type of transition involved. The D.C. two point probe method is used for resistivity and thermo electrical measurements.

3. Results and discussion

When precursor solution containing copper nitrate, ferrous sulphate, stannic chloride and thiourea was sprayed, a pyrolytic decomposition of precursor solution and formation of well-adherent CFTS thin films happened. The colour of TH10 was grey, with augmentation of thiourea contents in the precursor solution the colour of film became dark grey as seen from Fig. 1. The possible reaction mechanism for deposition of CFTS thin films can be written as follows:



Similar type of reaction has been presented by Patil et al. [27] for CZTS thin films. The film thicknesses of TH10, TH11, TH12, TH13, and TH14 estimated from gravimetric weight difference method were found to be 340 ± 20 nm.

3.1. Structural studies

XRD patterns of CFTS thin films spray deposited at 250 °C with various thiourea contents in the precursor solution are shown in Fig. 2. The polycrystalline crystal structure of the CFTS thin film is witnessed from XRD patterns. The diffraction peaks (112), (200), (004), (204), and (312) are detected at 2θ angles 28.25°, 32.85°, 33.37°, 47.51° and 55.99° respectively. These findings are in decent agreement with literature [28]. From JCPDS data card No. 44–1476, the matching of observed and standard 'd' values approve stannite phase of CFTS with tetragonal crystal structure (space group I-42 m). Similar type of crystal structure has been reported by Miao and colleagues [29] for electrochemically deposited CFTS films and Chatterjee et al. [30] for SILAR prepared CFTS thin films, and Wang and colleagues [31] for Rb incorporated CFTS thin films synthesized by blade-coating method. The broad humps observed in Fig. 2 for TH10 and TH13 are due to the amorphous nature of the glass substrates. Moreover, as seen from the figure, with augmentation of thiourea contents in the precursor solution, the (204) diffraction peak became comparatively intense and sharper, due to improved crystallinity up to TH13, whereas the width of the (204) diffraction peak decreased. Above TH13, increase in thiourea

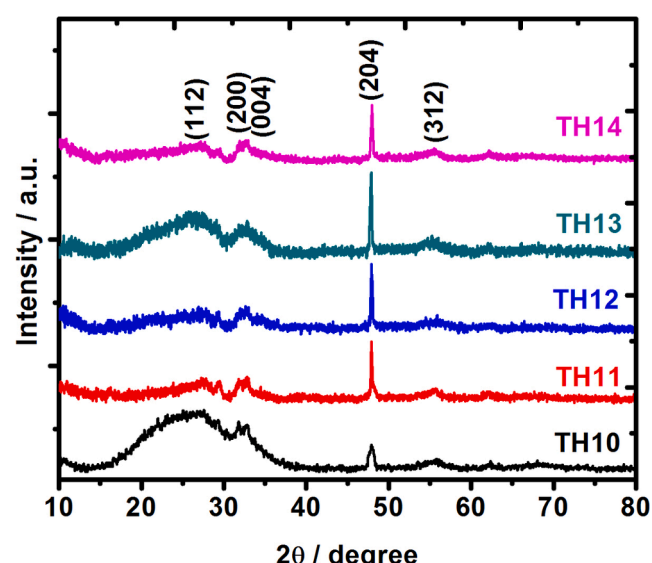


Fig. 2. XRD patterns of CFTS thin films spray deposited at 250 °C with various thiourea contents in the precursor solution.

Table 1
Structural data of spray deposited CFTS thin films.

Sample	2θ (°)	Observed d (Å)	Standard d (Å)	hkl	a = b (Å)	C (Å)	D (nm)	Tc (204)
TH10	27.56	3.233	3.157	112	5.63	10.74	18	0.63
	31.78	2.813	2.725	200				
	32.66	2.739	2.684	004				
	47.83	1.900	1.913	204				
	55.34	1.659	1.641	312				
TH11	27.26	3.268	3.157	112	5.63	10.35	23	2.01
	31.77	2.814	2.725	200				
	32.79	2.729	2.684	004				
	47.90	1.897	1.913	204				
	55.28	1.660	1.641	312				
TH12	27.24	3.271	3.157	112	5.45	10.75	29	2.11
	31.96	2.798	2.725	200				
	32.63	2.742	2.684	004				
	47.91	1.897	1.913	204				
	55.86	1.644	1.641	312				
TH13	27.34	3.259	3.157	112	5.62	10.62	35	2.47
	31.80	2.811	2.725	200				
	32.79	2.729	2.684	004				
	47.88	1.898	1.913	204				
	55.22	1.662	1.641	312				
TH14	27.15	3.281	3.157	112	5.60	10.48	30	2.11
	31.92	2.801	2.725	200				
	32.56	2.747	2.684	004				
	47.96	1.895	1.913	204				
	55.50	1.654	1.641	312				

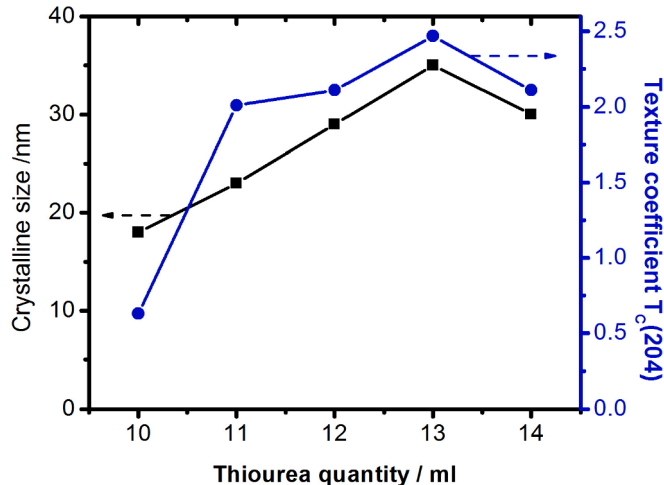


Fig. 3. Variation of crystalline size and texture coefficient $T_c(204)$ with thiourea contents in the precursor solution for spray deposited CFTS thin films.

contents in the precursor solution resulted in decrease in peak intensity which may be attributed to change in molecular plane for TH14 relative to the substrate plane. The lattice parameters ‘a’ and ‘c’ are calculated using standard relation [32]. The average lattice parameters are found to be $a = b = 5.58 \text{ \AA}$ and $c = 10.58 \text{ \AA}$ respectively, matching with standard JCPDS data ($a = b = 5.54 \text{ \AA}$ and $c = 10.73 \text{ \AA}$).

Crystalline size (D) was estimated using Debye Scherrer's formula [33]. Table 1 show crystalline sizes, it is observed that the crystalline size upsurges from 18 nm for TH10 with increase in thiourea contents in the precursor solution, reaches maximum to 35 nm for TH13 and decreases thereafter to 30 nm for TH14. The initial rise in crystalline size with increase in thiourea contents in the precursor solution up to TH13 is due to increase in adsorption sites up to TH13. Jiang and colleagues [14] have reported that a large crystalline size results in increased carrier diffusion length and reduced carrier recombination at grain

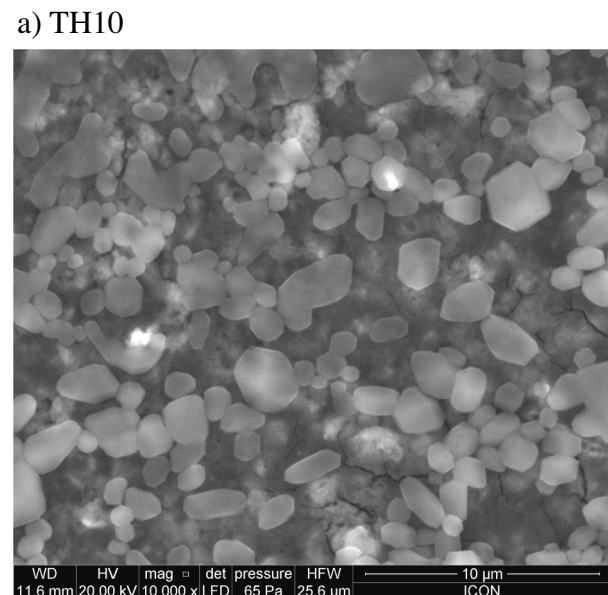
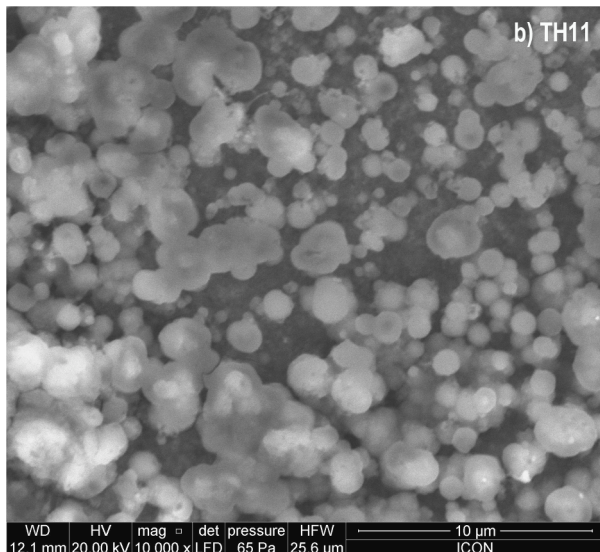


Fig. 4. SEM images of CFTS thin films spray deposited with various thiourea contents in the precursor solution (a) TH10, (b) TH11, (c) TH12, (d) TH13, and (e) TH14 respectively.

boundaries. Such thiourea concentration dependent crystalline size variation is also studied by Padmavathy et al. [34] for chemically deposited ZnS films and Youssef et al. [35] for zinc deposits. Above TH13, crystalline size decreases due to saturation of adsorption sites at the substrate surface [36].

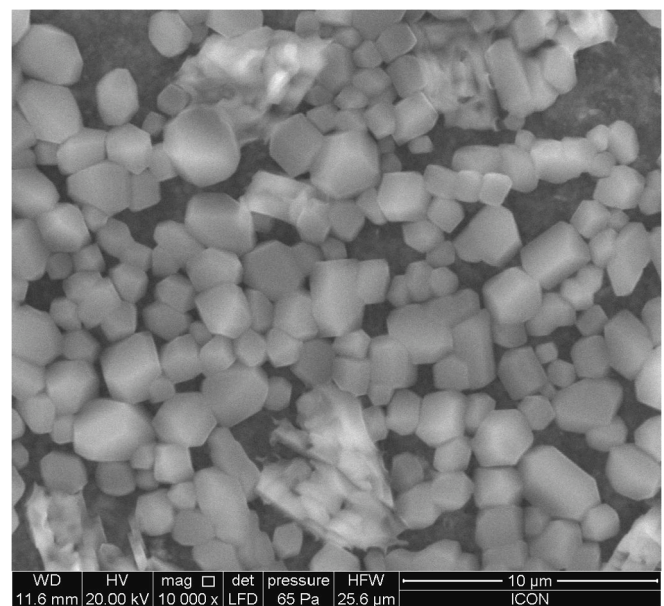
The influence of thiourea contents in the precursor solution on orientation of polycrystalline CFTS films was examined by computing the texture coefficients $T_c(hkl)$ [37]. Fig. 3 shows variation of crystalline size and texture coefficients $T_c(204)$ with thiourea contents in the precursor solution. From Table 1 and Fig. 3 it is witnessed that, with

**Fig. 4.** (continued)

rise in thiourea contents in the precursor solution, the texture coefficient reaches maximum for TH13 and decreases thereafter for TH14.

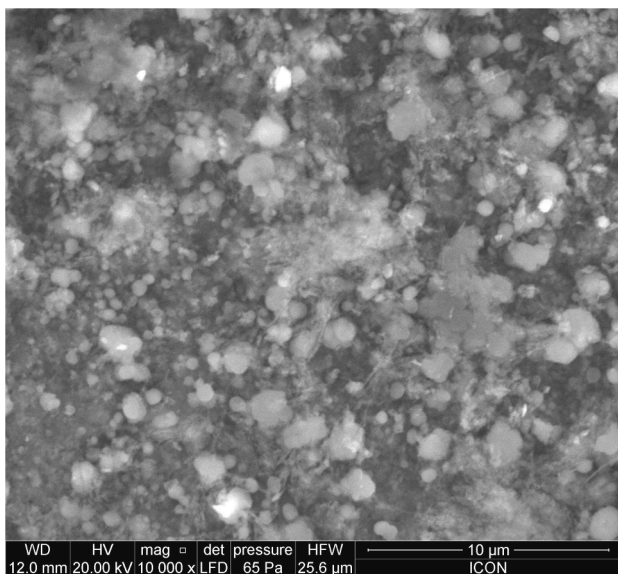
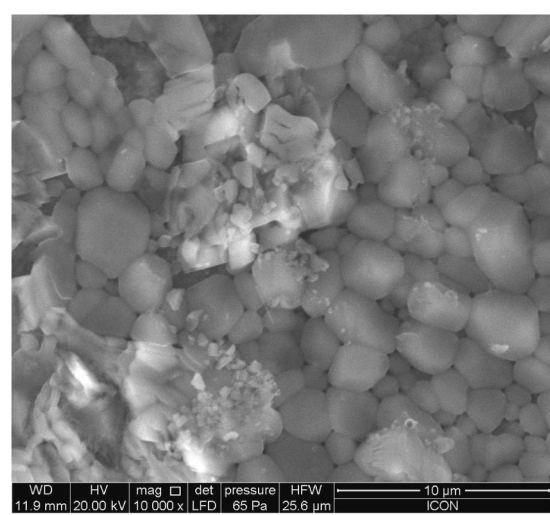
3.2. Surface morphological and compositional studies

Fig. 4 shows SEM pictures ($10,000\times$ magnifications) of CFTS thin films spray deposited with various thiourea contents in the precursor solution. It is evident that the beautiful hexagonal crystals of CFTS have been deposited uniformly. The SEM image of the TH10 sample consist of regular and irregular flakes of $1\text{--}2\,\mu\text{m}$, which change to thicker hexagonal crystals with upsurge in thiourea contents in the precursor solution. SEM image of TH14 consist of more packed hexagonal crystals with uniform distribution of constituents over the entire area of the film. The thiourea contents in the precursor solution play a significant role in defining the surface properties including grain distribution and

d) TH13**Fig. 4.** (continued)

porosity. Similar hexagonal plates type morphology was obtained by Kevin and co-workers for $\text{Cu}_2\text{FeSn}(\text{S},\text{Se}_{1-x})_4$ films [38]. It is resolved that augmentation of thiourea in the precursor solution is useful for refining surface morphology. The number of voids and larger hexagonal crystals observed are beneficial for applications of CFTS thin films in Photovoltaics [39].

Fig. 5 displays EDAX spectrum of CFTS films spray deposited with various thiourea contents in the precursor solution. It indicates peaks corresponding to Cu, Fe, Sn and S confirming CFTS phase. **Table 2** depicts elemental analysis of CFTS thin films spray deposited with various thiourea contents in the precursor solution. EDAX analysis shows atomic ratio of Cu, Fe, Sn and S are closer to 2:1:1:4 designating

c) TH12**Fig. 4.** (continued)**e) TH14****Fig. 4.** (continued)

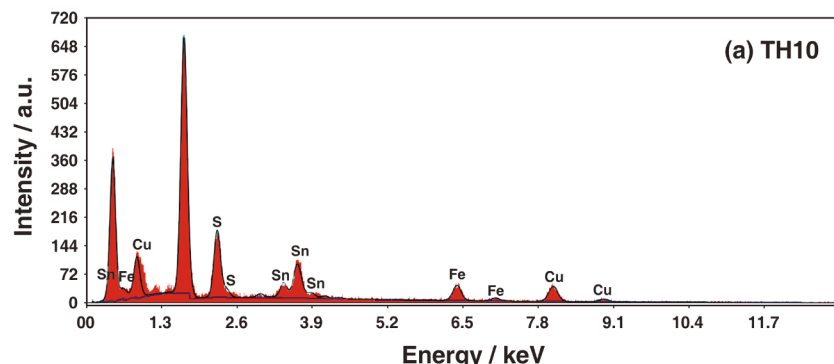


Fig. 5. EDAX patterns of CFTS thin films spray deposited with various thiourea contents in the precursor solution (a) TH10, (b) TH11, (c) TH12, (d) TH13, and (e) TH14 respectively.

nearly stoichiometric deposition of CFTS thin films for TH12 and TH13 samples.

3.3. Optical studies

Fig. 6 (a) depicts the absorbance spectra for CFTS thin films spray deposited with various thiourea contents in the precursor solution. The absorbance values were increased with the increase of thiourea contents in the precursor solution in UV–Vis region. Similar aspect of absorbance spectra have been observed in the literature [40]. Obaid et al. [41] have explained this behaviour by increasing number of atoms in thicker films making more states available for the absorption of photon energy. For TH13, we have a comparable absorbance, fine crystallinity, morphology and purity phase. These results display the responsiveness of CFTS thin films to absorption in the visible range. In crystalline semiconductors, the absorption coefficient ‘ α ’ and incident photon energy $h\nu$ are related through Tauc’s relation [42]. It is found that CFTS thin films have high coefficient of absorption 10^4 cm^{-1} in the visible region, indicating suitability of CFTS thin films for optoelectronic applications [43]. The plots of $(\alpha h\nu)^2$ versus $h\nu$ for CFTS thin films spray deposited with various thiourea contents in the precursor solution are shown in Fig. 6(b). The linear nature of plot specifies direct allowed type transition. It is witnessed that band gap widens with increase in thiourea contents in the precursor solution. Table 3 shows the band gap energies. The band gap energies are 1.54 eV, 1.61 eV, 1.66 eV, 1.71 eV and 1.76 eV for TH10, TH11, TH12, TH13 and TH14 respectively. The increase in band gap energies with thiourea contents in the precursor solution is due to the stimulus of various factors including crystalline size observed from XRD pattern, presence of impurities, carrier concentration, and deviation from stoichiometry [34]. Here, we consider that the observed variation in Eg is due to the change in crystalline size (Table 1). These values lie in the ideal range of band gap of absorber material for thin film solar cells [44,45] and consequently CFTS is useful in thin film solar cells. The variation of band gap energy with thiourea contents in the precursor solution for spray deposited CFTS thin films is shown in Fig. 6(c). Similar behaviour that is widening of band gap with increase in thiourea contents has been reported by Zia and colleagues for CdS-nanocrystalline thin films [46].

3.4. Electrical resistivity

The variation of $\log \rho$ versus inverse of absolute temperature for CFTS thin films spray deposited with various thiourea contents in the precursor solution is presented in Fig. 7. The reduction in electrical

resistivity with increase in temperature specifies typical semi-conducting behaviour. From Fig. 7 it is observed that, as the thiourea contents in the precursor solution upsurges the resistivity decreases for CFTS thin films up to TH13 and increases further for TH14. The room temperature electrical resistivity for TH10 is $0.646 \times 10^5 \Omega\text{cm}$, which decrease to $0.038 \times 10^5 \Omega\text{cm}$ (TH13) with increase in thiourea contents in the precursor solution and further increase to $0.070 \times 10^5 \Omega\text{cm}$ for TH14. The fall in the electrical resistivity with increase in thiourea contents is accredited to an increased free carrier concentration due to the incorporation of S^{2-} ions. The lower resistivity at TH13 may be associated to the better crystallinity which is related to the increase of grain size and preferred orientation [47]. According to Ozta et al. [48], the average grain size increases due to decrease of grain boundary areas. For TH14 sample, the free carrier concentration saturates and the mobility falls affecting the electrical resistivity. Similar behaviour was reported by Nieto-Zepeda et al. [40] for CdS thin films.

The activation energies (E_a) are determined using the Arrhenius equation [49]. The activation energies for low temperature zone were 0.09–0.12 eV and for high temperature zone were 0.31–0.37 eV respectively. Table 3 shows electrical resistivities and activation energies for CFTS thin films spray deposited with various thiourea contents in the precursor solution.

3.5. Thermoelectrical studies

The type of electrical conductivity possessed by the CFTS thin films spray deposited with various thiourea contents in the precursor solution is determined from thermoelectric power (TEP) measurement. Fig. 8 shows variation of thermo-emf with temperature difference (T) for CFTS thin films spray deposited with various thiourea contents in the precursor solution. The polarity of thermo-emf was negative towards hot end with respect to cold end, which confirms the fact that CFTS thin films spray deposited with various thiourea contents in the precursor solution are of p-type.

4. Conclusions

In conclusion, the influence of thiourea contents in the precursor solution on the properties of spray-deposited CFTS thin films was examined. XRD study showed tetragonal stannite crystal structure. Moreover, the crystallinity of the CFTS thin films enhanced with the augmentation of thiourea contents in the precursor solution. The large hexagonal crystals observed through SEM are beneficial in photovoltaic applications. EDAX study confirmed nearly stoichiometric deposition of

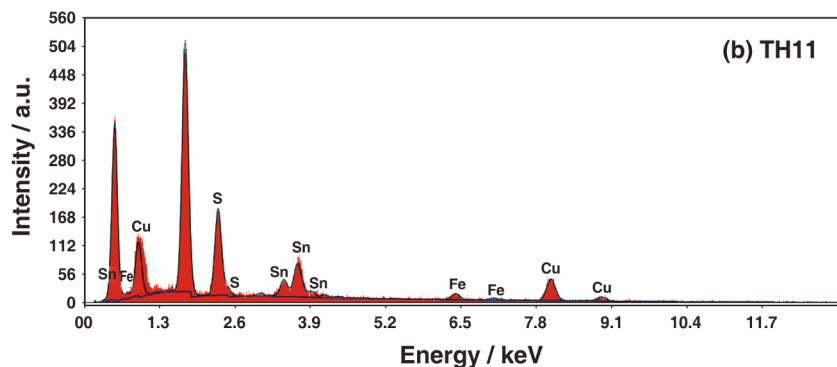


Fig. 5. (continued)

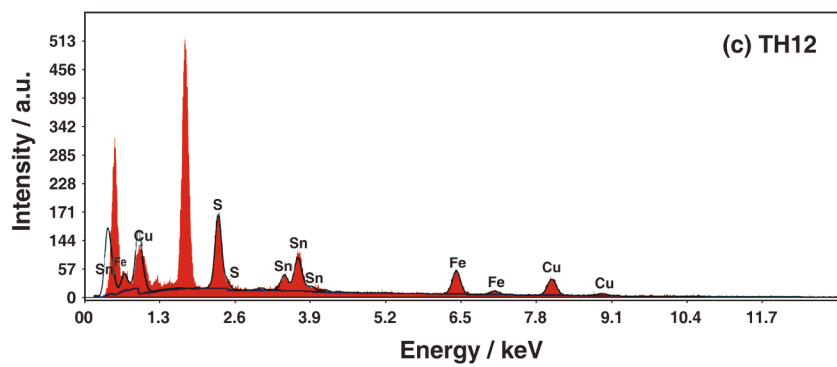


Fig. 5. (continued)

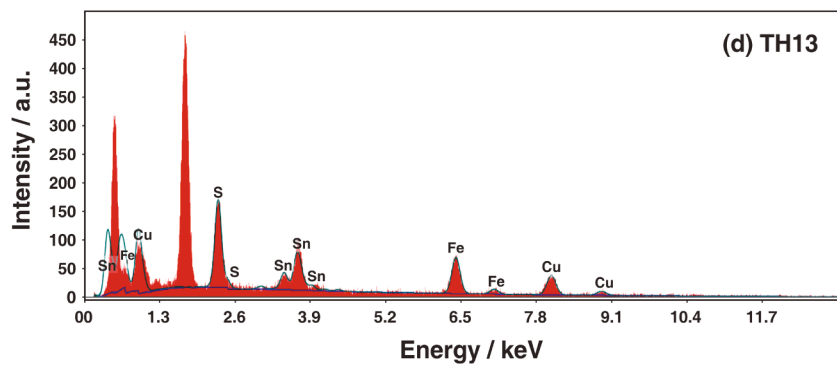


Fig. 5. (continued)

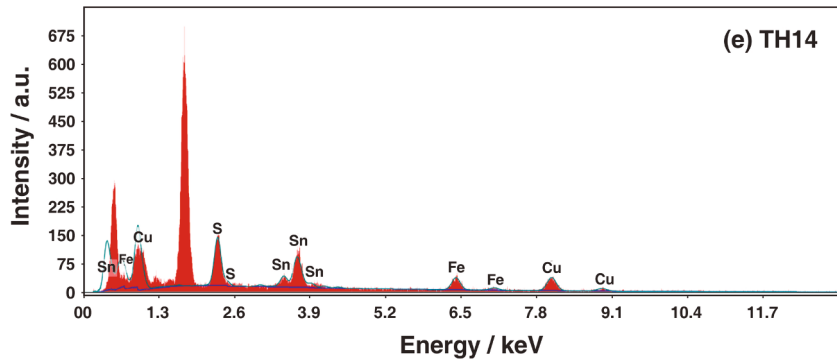


Fig. 5. (continued)

Table 2
Elemental analysis of spray deposited of CFTS thin films.

Sample	Atomic percentage in film by EDAX analysis (%)			
	Cu	Fe	Sn	S
Ideal	25.00	12.50	12.50	50.00
TH10	25.94	12.42	12.34	49.30
TH11	25.51	12.25	12.43	49.81
TH12	25.17	12.04	12.32	50.47
TH13	24.73	12.31	12.33	50.63
TH14	24.51	11.83	11.65	52.01

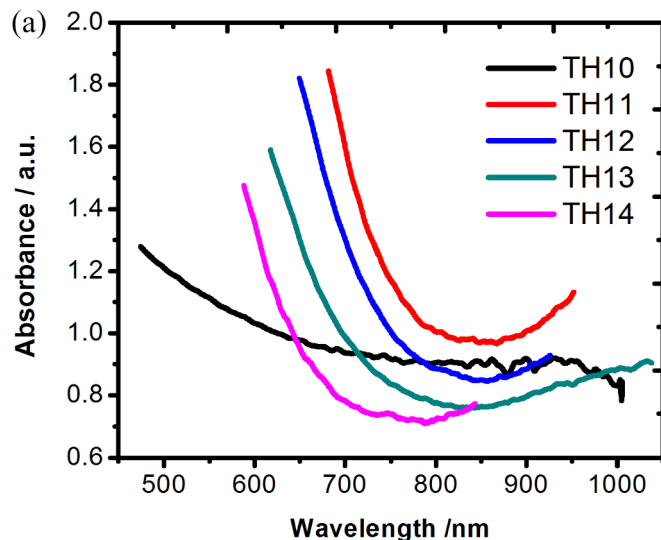


Fig. 6. (a) Absorbance spectra for CFTS thin films spray deposited with various thiourea contents in the precursor solution. 6(b) Variation of $(\alpha h\nu)^2$ versus $h\nu$ for CFTS thin films spray deposited with various thiourea contents in the precursor solution. 6(c) Variation of band gap energy with thiourea contents in the precursor solution for spray deposited CFTS thin films.

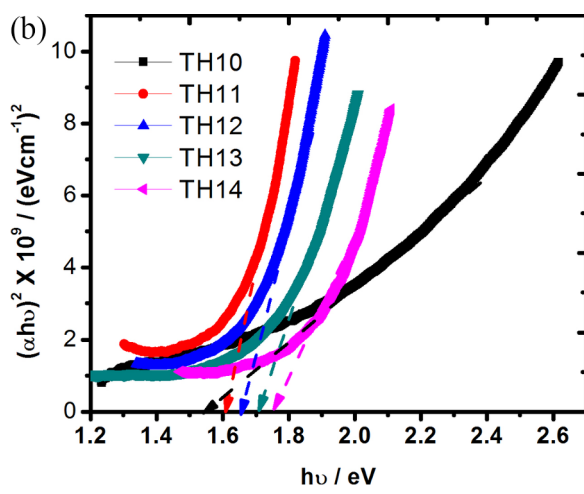


Fig. 6. (continued)

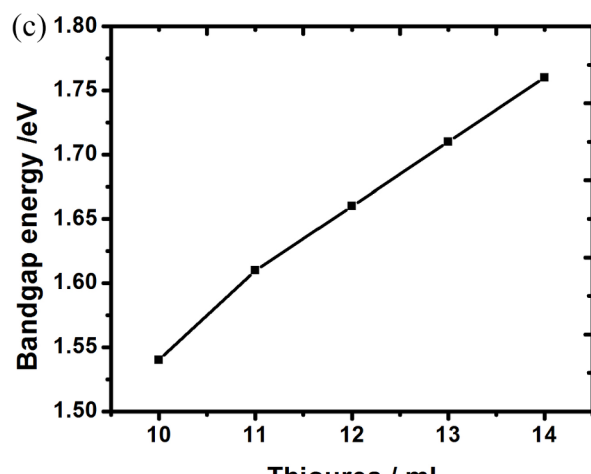


Fig. 6. (continued)

Table 3

Optical and electrical parameters of spray deposited of CFTS thin films.(R.T. – room temperature; L.T. - low temperature; H.T. - high temperature).

Sample	Band gap (Eg) (eV)	Electrical resistivity (ρ)		Activation energy (Ea)	
		R.T. ($\times 10^5 \Omega$ cm)	H.T. ($\times 10^1 \Omega$ cm)	(eV) H.T.	(eV) L.T.
TH10	1.54	0.646	3.10	0.31	0.12
TH11	1.61	0.295	2.09	0.36	0.11
TH12	1.66	0.123	1.48	0.38	0.10
TH13	1.71	0.038	0.56	0.33	0.09
TH14	1.76	0.070	0.82	0.37	0.09

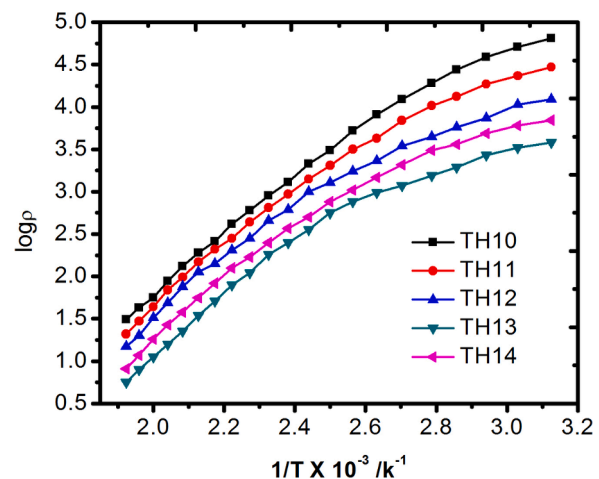


Fig. 7. Variation of $\log \rho$ versus inverse of absolute temperature for CFTS thin films spray deposited with various thiourea contents in the precursor solution.

CFTS thin films. The band gap energies of the CFTS thin films are quite close to the optimum value for a semiconductor material as an absorber layer in thin film solar cells. The electrical resistivity measurements

indicated typical semiconducting behaviour. The thermoelectrical analysis showed that CFTS thin films are p-type. It is concluded that quaternary CFTS with proper contents of thiourea in the precursor solution will show optimal performance for the photovoltaic applications.

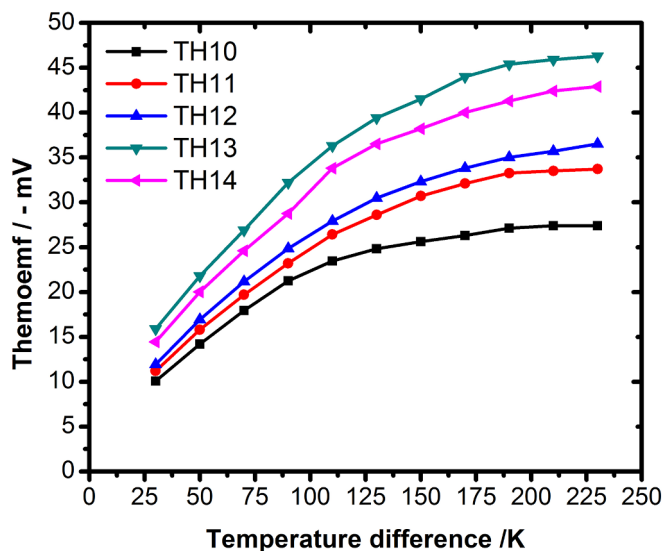


Fig. 8. Plot of thermoemf vs. temperature difference for CFTS thin films spray deposited with various thiourea contents in the precursor solution.

Declaration of interests

None.

References

- [1] H. Ahmoum, M. Boughrara, M.S. Su'ait, S. Chopra, M. Kerouad, Impact of position and concentration of sodium on the photovoltaic properties of zinc oxide solar cells, *Physica B* 560 (2019) 28–36.
- [2] Huafei Guo, Yan Li, Xiaohai Guo, Ningyi Yuan, Jianning Ding, Effect of silicon doping on electrical and optical properties of stoichiometric $\text{Cu}_2\text{ZnSnS}_4$ solar cells, *Physica B* 531 (2018) 9–15.
- [3] A. Bosio, G. Rosa, N. Romeo, Past, present and future of the thin film CdTe/CdS solar cells, *Sol. Energy* 175 (2018) 31–43.
- [4] Ait Aicha Youssef, Si Mohamed Bouziane, Zakaria Mohyi Eddine Fahim, Isa Sidir, Mohamed Hamidi, Mohammed Bouachrine, Designing Donor-Acceptor thienopyrazine derivatives for more efficient organic photovoltaic solar cell: a DFT study, *Physica B* 560 (2019) 111–125.
- [5] Taesoo D. Lee, Abasifreke U. Ebong, A review of thin film solar cell technologies and challenges, *Renew. Sustain. Energy Rev.* 70 (2017) 1286–1297.
- [6] Mpilo Wiseman Dlamini, Genene Tessema Mola, Near-field enhanced performance of organic photovoltaic cells, *Physica B* 552 (2019) 78–83.
- [7] S. Thiruvengadam, P. Sakthi, S. Prabhakaran, Sujay Chakravarty, V. Ganeshan, A. Leo Rajesh, Deposition and characterization of spray pyrolysed p-type Cu_2SnS_3 thin film for potential absorber layer of solar cell, *Physica B* 538 (2018) 8–12.
- [8] Y.H. Wang, X.Y. Zhang, N.Z. Bao, B.P. Lin, A. Gupta, Synthesis of shape-controlled monodisperse wurtzite $\text{CuIn}_x\text{Ga}_{1-x}\text{S}_2$ semiconductor nanocrystals with tunable band gap, *J. Am. Chem. Soc.* 133 (2011) 11072–11075.
- [9] Mohammad Reza Sayed Mir, Mohammad Esmail Yazdanshenas, Hakimeh Zare, Synthesis of color-tunable CdTe/CdS:Mn core-shell nanocrystal emitters, *Physica B* 557 (2019) 23–26.
- [10] B. Anderson, Materials availability for large-scale thin-film Photovoltaics, *Prog. Photovoltaics Res. Appl.* 8 (2000) 61–76.
- [11] Sreekanth Mandati, Suhash R. Dey, Shrikant V. Joshi, Bulusu V. Sarada, Two-dimensional $\text{CuIn}_{1-x}\text{Ga}_x\text{Se}_2$ nano-flakes by pulse electrodeposition for photovoltaic applications, *Sol. Energy* 181 (2019) 396–404.
- [12] Xiaoyan Zhang, Ningzhong Bao, Karthik Ramasamy, Yu-Hsiang A. Wang, Yifeng Wang, Baoping Lin, Arunava Gupta, Crystal phase-controlled synthesis of $\text{Cu}_2\text{FeSnS}_4$ nanocrystals with a band gap of around 1.5 eV, *Chem. Commun.* 48 (2012) 4956–4958.
- [13] Yan Chang, Chun Huang, Yang Jia, Fangyang Liu, Jin Liu, Yanqing Lai, Jie Li, Yexiang Liu, Synthesis and characterizations of quaternary $\text{Cu}_2\text{FeSnS}_4$ nanocrystals, *Chem. Commun.* 48 (2012) 2603–2605.
- [14] Xin Jiang, Wei Xu, Ruiqin Tan, Weijie Song, Jianmin Chen, Solvothermal synthesis of highly crystallized quaternary chalcogenide $\text{Cu}_2\text{FeSnS}_4$ particles, *Mater. Lett.* 102–103 (2013) 39–42.
- [15] Li Liang, Xiuyong Liu, Jan Huang, Meng Cao, Linjun Wang, Solution-based synthesis and characterization of $\text{Cu}_2\text{FeSnS}_4$ nanocrystals, *Mater. Chem. Phys.* 133 (2012) 688–691.
- [16] Achim Fischereder, Thomas Rath, Wernfried Haas, Heinz Amenitsch, Jörg Albering, Dorith Meischler, Sonja Larisegger, Michael Edler, Robert Saf, Ferdinand Hofer, Gregor Trimme, Investigation of $\text{Cu}_2\text{ZnSnS}_4$ formation from metal salts and thiouacetamide, *Chem. Mater.* 22 (2010) 3399–3406.
- [17] F.Z. Boutebakh, A. Beloucif, M.S. Aida, A. Chettah, N. Attaf, Zinc molarity effect on $\text{Cu}_2\text{ZnSnS}_4$ thin film properties prepared by spray pyrolysis, *J. Mater. Sci. Mater. Electron.* 29 (2018) 4089–4095.
- [18] Amrut Agasti, Sudhanshu Mallick, Parag Bhargava, Electrolyte pH dependent controlled growth of co-electrodeposited CZT films for application in CZTS based thin film solar cells, *J. Mater. Sci. Mater. Electron.* 29 (2018) 4065–4074.
- [19] Xian kuan Meng, Hong mei Deng, Jun He, Liping Zhu, Lin Sun, Ping xiong Yang, Junhao Chua, Synthesis of $\text{Cu}_2\text{FeSnS}_4$ thin film by selenization of RF magnetron sputtered precursor, *Mater. Lett.* 117 (2014) 1–3.
- [20] Bin lei Zhang, Meng Cao, Li Liang, Yan Sun, Yue Shen, Linjun Wang, Facile synthesis of $\text{Cu}_2\text{FeSnS}_4$ sheets with a simple solvothermal method, *Mater. Lett.* 93 (2013) 111–114.
- [21] Anima Ghosh, Amrita Biswas, Rajalingam Thangave, G. Udayabhanu, Photo-electrochemical properties and electronic band structure of kesterite copper chalcogenide $\text{Cu}_2\text{II-Sn}_4$ (II = Fe, Co, Ni) thin films, *RSC Adv.* 6 (2016) 96025–96034.
- [22] Lunhong Ai, Jing Jiang, Hierarchical porous quaternary Cu–Fe–Sn–S hollow chain microspheres: rapid microwave nonaqueous synthesis, growth mechanism, and their efficient removal of organic dye pollutant in water, *J. Mater. Chem.* 22 (2012) 20586–20592.
- [23] Wolfgang G. Zeier, Yanzhong Pei, Gregory Pomrehn, Tristan Day, Nicholas Heinz, Christophe P. Heinrich, G. Jeffrey Snyder, Wolfgang Tremel, Phonon scattering through a local anisotropic structural disorder in the thermoelectric solid solution $\text{Cu}_2\text{Zn}_{1-x}\text{Fe}_x\text{GeSe}_4$, *J. Am. Chem. Soc.* 135 (2013) 726–732.
- [24] M. Adelifard, Preparation and characterization of $\text{Cu}_2\text{FeSnS}_4$ quaternary semiconductor thin films via the spray pyrolysis technique for photovoltaic applications, *J. Anal. Appl. Pyrolysis* 122 (2016) 209–215.
- [25] Rajiv Ramanujam Prabhakar, Nguyen Huu Loc, Mulumudi Hemant Kumar, Pablo P. Boix, Sun Juan, Rohit Abraham John, Sudip K. Batabyal, Lydia Helena Wong, Facile water-based spray pyrolysis of earth-abundant $\text{Cu}_2\text{FeSnS}_4$ thin films as an efficient counter electrode in dye-sensitized solar cells, *ACS Appl. Mater. Interfaces* 6 (2014) 17661–17667.
- [26] S.G. Nilange, N.M. Patil, A.A. Yadav, Growth and characterization of spray deposited quaternary $\text{Cu}_2\text{FeSnS}_4$ semiconductor thin films, *Physica B* 560 (2019) 103–110.
- [27] S.J. Patil, V.C. Lokhande, Dong-Weon Lee, C.D. Lokhande, Electrochemical impedance analysis of spray deposited CZTS thin film: effect of Se introduction, *Opt. Mater.* 58 (2016) 418–425.
- [28] Jicheng Zhou, Zhibin Ye, Yunyun Wang, Qiang Yi, Jiawei Wen, Solar cell material $\text{Cu}_2\text{FeSnS}_4$ nanoparticles synthesized via a facile liquid reflux method, *Mater. Lett.* 140 (2015) 119–122.
- [29] Xiaohui Miao, Ruizhi Chen, Wenjuan Cheng, Synthesis and characterization of $\text{Cu}_2\text{FeSnS}_4$ thin films prepared by electrochemical deposition, *Mater. Lett.* 193 (2017) 183–186.
- [30] Soumyo Chatterjee, Amlan J. Pal, A solution approach to p-type $\text{Cu}_2\text{FeSnS}_4$ thin-films and pn-junction solar cells: role of electron selective materials on their performance, *Sol. Energy Mater. Sol. Cells* 160 (2017) 233–240.
- [31] Shuo Wang, Ruixin Ma, Chengyan Wang, Shina Li, Hua Wang, Incorporation of Rb cations into $\text{Cu}_2\text{FeSnS}_4$ thin films improves structure and morphology, *Mater. Lett.* 202 (2017) 36–38.
- [32] D.B. Khadka, Jun Ho Kim, Structural, optical and electrical properties of Cu_2FeSn_4 (X = S, Se) thin films prepared by chemical spray pyrolysis, *J. Alloys Compd.* 638 (2015) 103–108.
- [33] A.A. Yadav, Nanocrystalline copper selenide thin films by chemical spray pyrolysis, *J. Mater. Sci. Mater. Electron.* 25 (2014) 1251–1257.
- [34] V. Padmavathy, S. Sankar, V. Ponnuwamy, Influence of thiourea on the synthesis and characterization of chemically deposited nanostructured zinc sulphide thin films, *J. Mater. Sci. Mater. Electron.* 29 (2018) 7739–7749.
- [35] Kh.M.S. Youssef, C.C. Koch, P.S. Fedkiw, Influence of additives and pulse electrodeposition parameters on production of nanocrystalline zinc from zinc chloride electrolytes, *J. Electrochem. Soc.* 151 (2004) C103–C111.
- [36] Y.B. Kishore Kumar, P. Uday Bhaskar, G. Suresh Babu, V. Sundara Raja, Effect of copper salt and thiourea concentrations on the formation of $\text{Cu}_2\text{ZnSnS}_4$ thin films by spray pyrolysis, *Phys. Status Solidi A* 207 (2010) 149–156.
- [37] A.A. Yadav, M.A. Barote, T.V. Chavan, E.U. Masumdar, Influence of indium doping on the properties of spray deposited $\text{CdS}_{0.8}\text{Se}_{0.2}$ thin films, *J. Alloys Compd.* 509 (2011) 916–921.
- [38] Punarja Kevin, M. Azad Malik, Paul O'Brien, The AACVD of $\text{Cu}_2\text{FeSn}(\text{S},\text{Se}_{1-x})_4$: potential environmentally benign solar cell materials, *New J. Chem.* 39 (2015) 7046–7053.
- [39] Peter Baláž, Matej Baláž, Maríja J. Sayagués, Ivan Škorvánek, Anna Zorkovská, Erika Dutková, Jaroslav Briančin, Jaroslav Kováč, Jaroslav Kováč, Jaroslav Špotyuk, Mechanochemical solvent-free synthesis of quaternary semiconductor $\text{Cu}-\text{Fe}-\text{Sn}-\text{S}$ nanocrystals nano, *Res. Lett.* 12 (2017) 256–266.
- [40] K.E. Nieto-Zepeda, A. Guillén-Cervantes, K. Rodríguez-Rosales, J. Santos-Cruz, D. Santos-Cruz, M. de la L. Olvera, O. Zelaya-Ángel, J. Santoyo-Salazar, L.A. Hernández-Hernández, G. Contreras-Puente, F. de Moure-Flores, Effect of the sulfur and fluorine concentration on physical properties of CdS films grown by chemical bath deposition, *Results Phys.* 7 (2017) 1971–1975.
- [41] A.S. Obaid, M.A. Mahdi, Y. Yusof, M. Bououdina, Z. Hassan, Structural and optical properties of nanocrystalline lead sulfide thin films prepared by microwave-assisted chemical bath deposition, *Mater. Sci. Semicond. Process.* 16 (2013) 971–979.
- [42] X.L. Tong, D.S. Jiang, W.B. Hu, Z.M. Liu, M.Z. Lout, The comparison between CdS thin films grown on Si(111) substrate and quartz substrate by femtosecond pulsed laser deposition, *Appl. Phys. A* 84 (2006) 143–148.
- [43] Nader Ghobadi, Strong localization of the charge carriers in CdSe nanostructural

- films, *Int. Nano Lett.* 3 (2013) 47–52.
- [44] Sharadrao A. Vanalakar, Satish M. Patil, Vithoba L. Patil, Sagar A. Vhanalkar, Pramod S. Patil, Jin H. Kim, Simplistic eco-friendly preparation of nanostructured $\text{Cu}_2\text{FeSnS}_4$ powder for solar photocatalytic degradation, *Mater. Sci. Eng. B* 229 (2018) 135–143.
- [45] Xiankuan Meng, Hongmei Deng, Jiahua Tao, Huiyi Cao, Xinran Li, Lin Sun, Pingxiong Yang, Junhao Chu, Heating rate tuning in structure, morphology and electricity properties of $\text{Cu}_2\text{FeSnS}_4$ thin films prepared by sulfurization of metallic precursors, *J. Alloys Compd.* 680 (2016) 446–451.
- [46] Rehana Zia, Madeeha Riaz, Quratul ain, Safia Anjum, Study the effect of thiourea concentration on optical and structural properties of CdS-nanocrystalline thin films prepared by CBD technique, *Optik* 127 (2016) 5407–5412.
- [47] Chayma Nefzi, Mehdi Souli, Yvan Cuminal, Najoua Kamoun-Turki, Effect of sulfur concentration on structural, optical and electrical properties of $\text{Cu}_2\text{FeSnS}_4$ thin films for solar cells and photocatalysis applications, *Superlattice. Microst.* 124 (2018) 17–29.
- [48] Mustafa Ozta, Influence of grain size on electrical and optical properties of InP films, *Chin. Phys. Lett.* 25 (2008) 4090–4092.
- [49] A.S. Hassanien, Alaa A. Akl, Effect of Se addition on optical and electrical properties of chalcogenide CdSSe thin films, *Superlattice. Microst.* 89 (2016) 153–169.